HE 1.2.28

ENERGY DEPOSITION OF 10 TeV HADRONS IN THE KASCADE CALORIMETER

J. Milke* for the KASCADE Collaboration†

Forschungszentrum Karlsruhe, Institut für Kernphysik, D-76021 Karlsruhe, Germany

ABSTRACT

Using the central large hadron calorimeter of the KASCADE experiment, single hadrons have been investigated. Experiences concerning the stability of performance and uniformity of response are discussed. In detail the transition curves of energy deposition in the iron absorber have been studied up to 10 TeV, especially in view of unexpected phenomena. No indication for a pronounced deviation is observed, the transition curves are described by the FLUKA program as implemented in GEANT code rather satisfactorily.

INTRODUCTION

For many decades, the study of cosmic rays concentrated on the composition and the spectrum of primary particle flux. At energies above 10^{14} eV, the experiments were mainly performed using a scintillator matrix at sea or mountain level to detect the electromagnetic and muonic components of extensive air showers (EAS) evolving from primary particles. As the fluctuations in an EAS are very large, it is important to observe not only the electromagnetic and muonic particles of the showers but the hadronic ones as well. Observing all components simultaneously allows the experimenter to evaluate correlations and to infer more stringently the primary's identity and energy and even its interactions with air nuclei.

For this reason the KASCADE experiment has set up a large hadron calorimeter in the centre of an array for electron and muon detection to study the cores of EAS with high accuracy (Hörandel et al., 1997). Of this calorimeter 200 m^2 are operational since nearly one year. In the calorimeter the hadrons interact in an absorber block of iron slabs and deposit energy in the ionisation chambers interspersed between the absorbers.

When passing the atmosphere of about 10 nuclear interaction lengths λ_I thickness, a proton on average undergoes ten collisions before it reaches sea level, and loses part of its energy at each collision. As the inelasticity is ≈ 0.5, a primary particle retains a mean energy of $E_H \approx 10^{-3}\ E_0$ at observation level. There is, however, a small but non vanishing probability for a particle to undergo much fewer interactions or to lose much less than half of its energy, e.g. in a diffractive interaction. As the primary flux rises rapidly with falling energy, there is a significant chance to find a hadron that has penetrated the atmosphere without having lost much energy and that has reached ground level as an almost unaccompanied particle. With these single hadrons the performance of the calorimeter is monitored continuously and the studies presented below have been undertaken.

THE APPARATUS

The set–up of the central KASCADE detector is sketched in Figure 1. The iron slabs are stacked on a concrete ceiling leaving 7 horizontal slots for the liquid ionisation chambers and one for scintillation counters. The latter serve as fast trigger elements both for the ionisation chambers and the multi-wire chambers below the ceiling in the basement. On top a 5 cm lead filter ensures an efficient absorption of the electromagnetic component shielding the first

*corresponding author, e-mail: milke@ik1.fzk.de

†A full list of authors and institutions of the KASCADE Collaboration is given at the end of this volume.

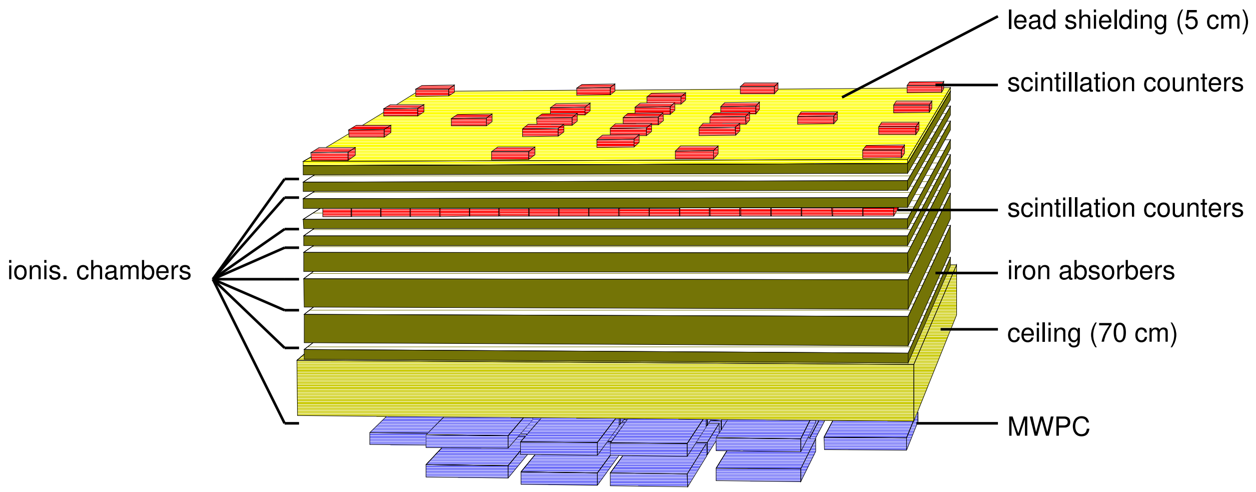

Fig. 1: Schematic view of the KASCADE central detector.

layer of chambers by 15 radiation lengths X_0. A scintillator matrix serves to trigger on the electromagnetic component. The total depth of the calorimeter corresponds to $11\lambda_I$.

A sketch of an ionisation chamber is presented in Figure 2, showing the segmentation of the electrodes to 25×25 cm^2, which are positioned in the midplane of the box by ceramic spacers and read out individually. The fine spatial segmentation allows to reconstruct hadron cascades separately and to determine their impact point, angle of incidence, and energy. The chambers are filled with the liquids tetramethylsilane or tetramethylpentane which are perfect insulators, but exhibit very good electron conductivity for excess electrons injected, e.g. by ionisation (Engler, 1996).

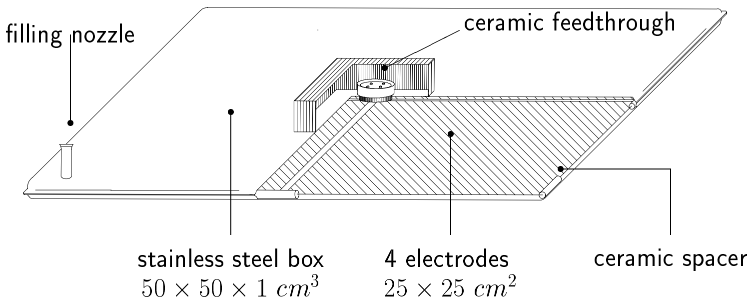

Fig. 2: Sketch of a liquid ionisation chamber filled with tetramethylsilane or tetramethylpentane.

Liquid ionisation chambers exhibit a very linear signal behavior. The dynamic range is limited by the electronics only, and amounts to $1 : 2 \times 10^4$. It is realized by a non-linear digital conversion characteristic for high pulses. Signals are recorded from a through-going muon (0.8 MeV energy deposition) up to 9 GeV energy deposition per channel in a high energy EAS without saturation. Hence, hadrons are detected up to 10 TeV without being restrained by saturation. For a 25 TeV hadron a 10% signal decrease by electronic saturation has to be accounted for.

For the present analysis 26 000 out of total 40 000 electronic channels have been operating. The relative calibration of all electronic channels is performed by a charge injection into the preamplifier input. Repeated overall checks reproduced the calibrations within $\pm 1\%$.

The high density of a liquid makes an absolute energy calibration feasible by using the energy deposition of muons. The muon signals are just above noise level and clearly visible in a summed-up spectrum of several particles. Prior to installation each chamber is calibrated in a test arrangement utilizing single penetrating muons. At an electric field of 10 keV/cm typically applied to the chambers, approximately 95% of the ionisation charge is collected.

RESPONSE MONITORING

One of the principal motivations to use liquid ionisation chambers for a ten year cosmic ray

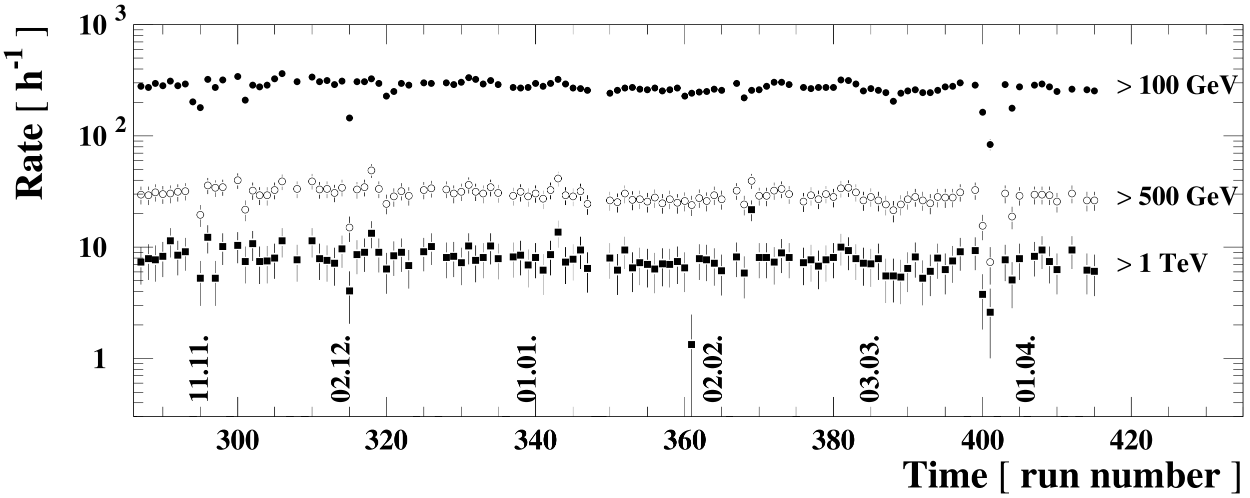

Fig. 3: Rate of reconstructed hadrons versus time. The data refer to the actual time of running in 1996 and 1997.

experiment is their long–term stability. The electronic feed–back amplifier chain fulfills this requirement. For the actual chamber signal, however, this has to be proven. The first experience with the calorimeter is documented in Figure 3. It shows the rate of hadrons versus time for three different energy thresholds of the detected particles. One observes a rather stable hadron rate. Due to the steeply falling energy spectrum a slight shift in the energy threshold would be noticeable immediately. The decrease around the run number 402 was caused by known technical reasons, and these runs are excluded from the analysis. As the lowest threshold 100 GeV has been chosen as for this energy the hadron recognition in the calorimeter reaches full efficiency. For the detailed efficiency curve see (Unger et al., 1997).

A further check upon proper operation of the calorimeter is a spatial survey of single hadrons. An example is presented in Figure 4. It shows as a scatter plot the points of traverse through the upper layer for all reconstructed hadrons above 100 GeV in a particular data run. The homogeneity reflects the appropriate function of all chambers. In fact, only 0.5% of the channels are malfunctioning, which is corrected for in the reconstruction algorithm.

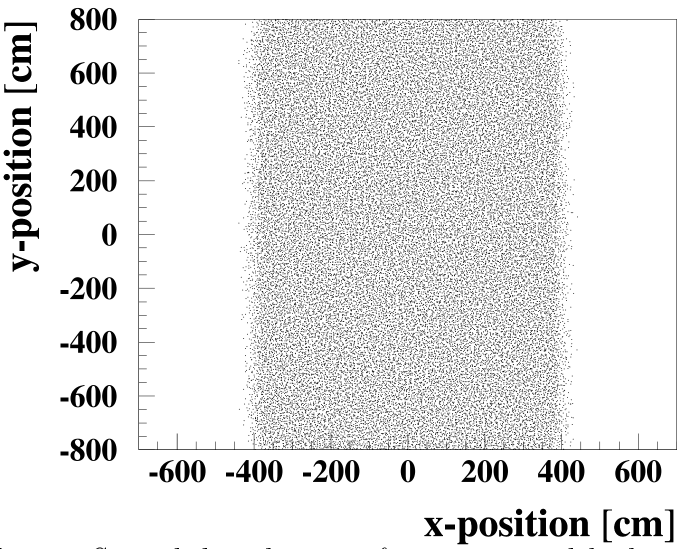

Fig. 4: Spatial distribution of reconstructed hadrons within the calorimeter.

TRANSITION CURVES

The energy assignment to a reconstructed shower relies on Monte Carlo predictions, because in the TeV region no direct calibration using an accelerator beam is feasible. The response for each of the chambers is calibrated using minimum ionising muons. The signal damping for densely ionising particles has been studied at the Karlsruhe cyclotron using deuterons and tritons (Engler et al., 1993). This signal saturation has been properly parameterized and implemented in the GEANT code. Calculations with both, FLUKA and GHEISHA, reproduce well the signal of low energy hadrons of a few GeV (Engler et al., 1992). In the TeV region, however, when attributing energy to a hadron on basis of its energy sum in the calorimeter, we cannot check whether the simulation predicts the correct energy deposit or not. We can, however, check whether the pattern of energy deposition in the calorimeter is correctly reproduced by the simulation.

For this purpose we compare the longitudinal distributions of showers with the same reconstructed energy deposit. In Figure 5 six transition curves for energies between 0.5 and 10 TeV are shown. Plotted is the average energy deposit versus the depth in the calorimeter together with simulations using the FLUKA program as implemented in the GEANT code. Cascades above 6 TeV have been processed by an additional eye scan in order to verify that no accompanying particles spoil the transition curves. As can be seen the simulations reproduce the experimental findings rather well within the error bars. Small deviations might be due to the way the inelastic cross–sections in iron are treated in FLUKA. In particular, no deviation of the experimental findings from the simulation can be found in the region $2.0 < \lambda_I < 5.5$, where (Yakovlev, 1992) has found indication of an unexplained flattening.

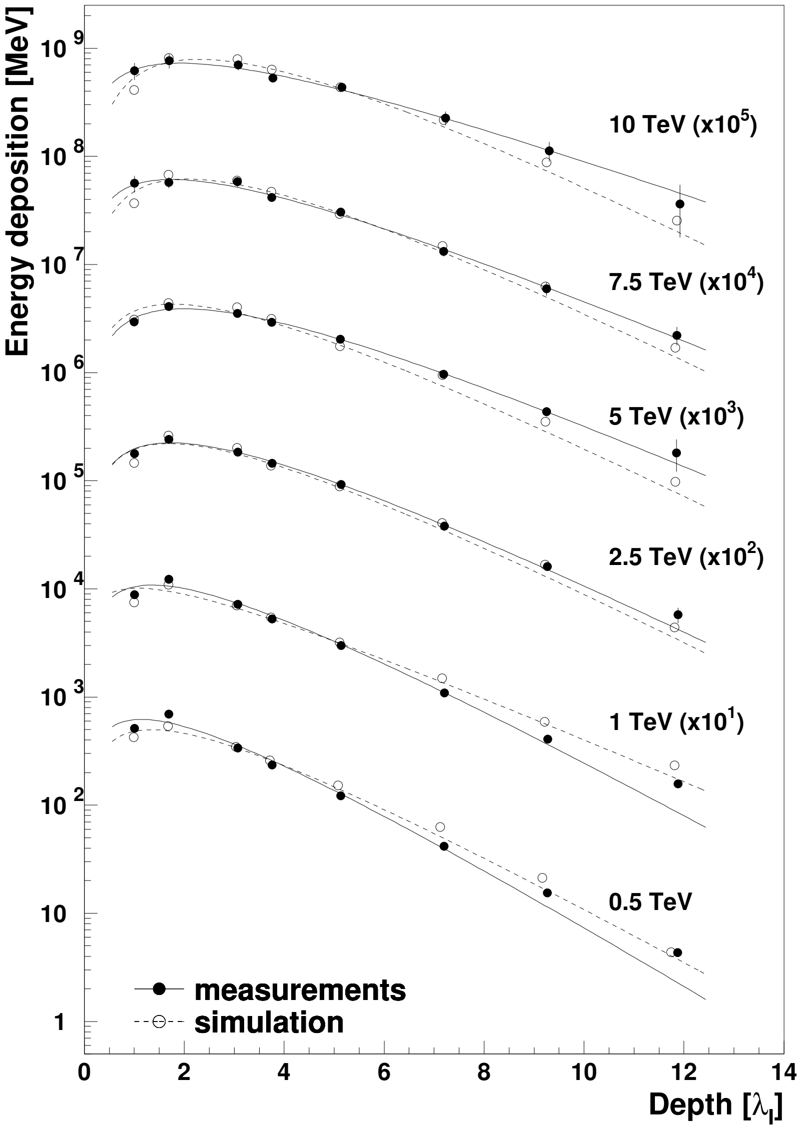

Fig. 5: Transition curves: Energy deposition versus depth in calorimeter. The energy depositions have been multiplied by the factor in the brackets. The curves represent fits of the data to $dE(\lambda) = c\,\lambda^a\, e^{-b\lambda}$.

CONCLUSION

The calorimeter of the KASCADE experiment works with satisfying performance and long–term stable response. The data are well reproduced by simulations with no unconventional physics involved. Improved statistics will enable an extension of the investigations to higher energies.

REFERENCES

Engler, J. et al., *Nucl. Instr. and Meth.*, **A20**, 460 (1992)

Engler, J. et al., *Nucl. Instr. and Meth.*, **A327**, 128 (1993)

Engler, J. et al., *J. Phys. G: Nucl. Part. Phys.*, **22**, 1 (1996)

Hörandel, J.R., et al., *Proc. 25th ICRC*, Durban, **HE 1.2.27** (1997)

Klages, H.O. et al., Nucl. Phys. B (Proc.Suppl), **52B**, 92, (1997)

Unger, J. et al., *Proc. 25th ICRC*, Durban, **HE 2.1.2** (1997)

Yakovlev, V.F., *AIP Conf. Proc. 276*, Ann Arbor, p. 154 (1992)